Acta Cryst. (1981). A37, 723–728

Crystal Structure Analysis of $Ca_4YFe_5O_{13}$ by Combining 1 MeV High-Resolution Electron Microscopy with Convergent-Beam Electron Diffraction

BY Y. BANDO,* Y. SEKIKAWA, H. YAMAMURA AND Y. MATSUI

National Institute for Researches in Inorganic Materials, 1-Namiki, Sakura-mura, Niihari-gun, Ibaraki 305, *Japan*

(*Received* 23 *December* 1980; *accepted* 16 *March* 1981)

Abstract

By combining 1 MeV high-voltage–high-resolution electron microscopy with convergent-beam electron diffraction (CBED), the crystal structure of a perovskite-related compound, $Ca_4YFe_5O_{13}$, is determined. The crystal has orthorhombic symmetry with lattice parameters $a = 5{\cdot}46$, $b = 37{\cdot}4$ and $c = 5{\cdot}54$ Å. The space group is determined to be centrosymmetric *Pnma* by selecting the point group from the CBED patterns. The structure images taken from two principle-axis directions, which are interpreted on the basis of the calculated images, reveal that the structure consists of a succession of the stacking of FeO_6 octahedra (*O* layer) and FeO_4 tetrahedra (*T* layer) and is represented by the stacking sequence of ...*OTOOTOTOOTO*... along the *b* axis repeated at intervals of 37·4 Å. It is shown that the $Ca_4YFe_5O_{13}$ crystal structure can be described in terms of unit-cell-level twinning of $Ca_2Fe_2O_5$.

Introduction

With the present day high-resolution electron microscope it is possible to carry out a structure analysis of a crystal by directly observing the arrangement of individual heavy atoms. The increased accelerating voltage allows more finely resolved structure images than 100 kV, because more scattered waves can be used for structure imaging. This will increase the accuracy of the crystal structure analysis. The 1 MeV high-voltage–high-resolution electron microscope at NIRM (Japan) can resolve a lattice spacing of about 2 Å at an accelerating voltage of 1 MeV with axial illumination and a goniometer stage (Horiuchi, Matsui & Bando, 1976). It has been demonstrated that 1 MeV high-resolution electron microscopy is very useful for the determination of crystal structures and many structures of inorganic compounds have been solved on the basis of electron diffraction patterns and finely resolved structure images taken along two or more directions, in which each cation site is resolved (Horiuchi, Kikuchi & Goto, 1977; Bando, Watanabe, Sekikawa, Goto & Horiuchi, 1979; Bando, Saeki, Sekikawa, Matsui, Horiuchi & Nakahira, 1979; Bando, Watanabe & Sekikawa, 1979, 1980; Matsui, Kato, Kimizuka & Horiuchi, 1979). For a $Bi_2W_2O_9$ crystal (Bando, Watanabe, Sekikawa, Goto & Horiuchi, 1979) the space group has been determined uniquely to be non-centrosymmetric $Pna2_1$ from the 1 MeV structure image in which each of the Bi and W atom sites is clearly resolved and the arrangement of these atoms shows the absence of the mirror symmetry perpendicular to the *c* axis, indicating that the point group is not *mmm* but *mm*2. This is a fortunate example because usually it seems to be difficult to select the true space group from the structure images coupled with the normal electron diffraction patterns.

On the other hand, convergent-beam electron diffraction (CBED) is a powerful method for determining the point group of crystals (Goodman, 1975; Buxton, Eades, Steeds & Rackham, 1976). Tanaka, Saito & Watanabe (1980) and Johnson & Gatehouse (1980) selected space groups uniquely by determining the point groups from the CBED patterns. Therefore, the combination of high-resolution electron microscopy and CBED should be very successful for crystal structure analysis. Recently, Goodman, Spence, Olsen & Roth (1980) tried this with 100 kV electron microscopy.

The oxygen-deficient perovskite-related compounds have been widely studied. Among them, the compounds in the system between perovskite $CaTiO_3$ and dicalcium ferrite $Ca_2Fe_2O_5$ have intermediate structures which can be represented by a succession of sheets of oxygen octahedra and oxygen tetrahedra along the *b* axis (Grenier, Darriet, Pouchard & Hagenmuller, 1976; Grenier, Schiffmacher, Caro, Pouchard & Hagenmuller, 1979). In this system, the tetravalent *B* cations in the perovskite ABO_3 are replaced by the trivalent cations Fe^{3+} in the dicalcium ferrite resulting in the formation of various stackings of the octahedra and

* Present address: Center for Solid State Science, Arizona State University, Tempe, AZ 85281, USA.

0567-7394/81/050723-06$01.00

tetrahedra. It is then expected that if trivalent A cations in the perovskite are replaced by divalent Ca^{2+} cations, the perovskite-related compounds mentioned earlier are also formed in the system $AFeO_3$–$Ca_2Fe_2O_5$, where A is Y, La and Ga (Grenier *et al.*, 1979). In a previous paper (Bando, Yamamura & Sekikawa, 1980), we reported a new compound $Ca_4YFe_5O_{13}$ in the system $YFeO_3$–$Ca_2Fe_2O_5$ and studied its crystal structure by one-dimensional lattice imaging and X-ray powder diffraction. However, the true space group and the framework of the crystal structure is still uncertain.

In this paper, we combine 1 MeV high-resolution electron microscopy with CBED to determine the crystal structure of the perovskite-related compound $Ca_4YFe_5O_{13}$. It is shown that the space group is selected uniquely by determining the point group from CBED. The images observed are interpreted with image calculation.

Experimental

The crystals were prepared by intimate mixing of graduated pure reagents ($CaCO_3$, Y_2O_3 and Fe_2O_3) and by firing at 1270 K for 15 h in air. The samples were then refired at 1570 K and quenched to room temperature. The starting composition of the crystals was $1{\cdot}6CaO.0{\cdot}2Y_2O_3.Fe_2O_3$. The products obtained contained small amounts of $Ca_2Fe_2O_5$.

The specimens thus prepared were crushed in an agate mortar to fragments of several micrometres in size. They were placed on a holey carbon supporting film and observed under the 1 MeV electron microscope. The accelerating voltage was 800 kV. The objective aperture size corresponded to about 0·5 $Å^{-1}$ in reciprocal space. The image contrast obtained at underfocus values between 500 and 1000 Å was interpreted on the basis of calculated images. The direct magnification was $2{\cdot}5 \times 10^5$ times and the exposure time was about 3 s.

The convergent-beam electron diffraction patterns were taken with a Philips 400 electron microscope operated at 120 keV accelerating voltage. The probe diameter was almost 200 Å at the crystal.

Results and interpretation

1. *Space-group determination by CBED*

Conventional electron diffraction patterns of $Ca_4YFe_5O_{13}$ crystal fragments are shown in Fig. 1(*a*) to (*c*). The crystal has orthorhombic symmetry with lattice parameters $a = 5{\cdot}46$, $b = 37{\cdot}4$ and $c = 5{\cdot}54$ Å, which were refined by X-ray powder diffraction. The systematic absent reflections are $0kl$ with $k + l = 2n + 1$, $hk0$ with $h = 2n + 1$. Therefore, the possible space

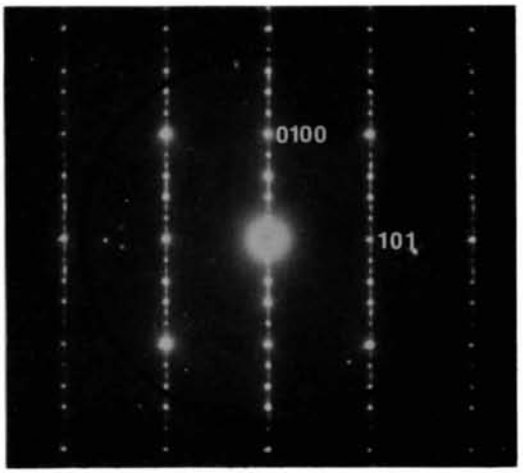

(*a*)

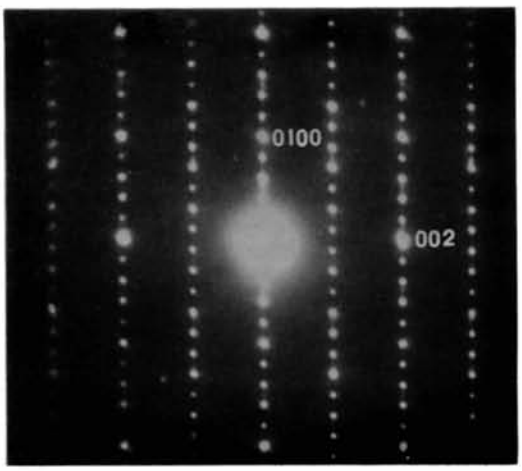

(*b*)

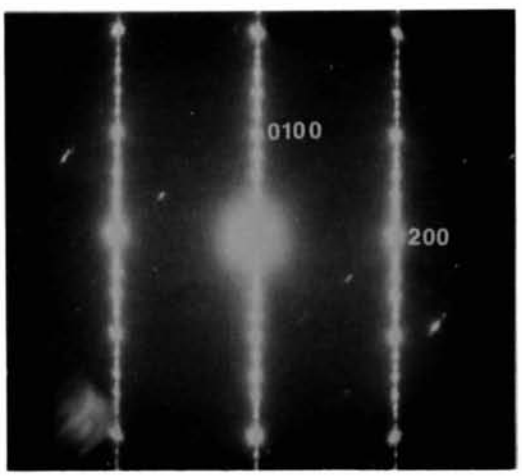

(*c*)

Fig. 1. Electron diffraction patterns taken from $Ca_4YFe_5O_{13}$ crystal fragments. The incident electron beam is parallel (*a*) to [10$\bar{1}$], (*b*) to [100] and (*c*) to [001]. The size and the position of the objective aperture is outlined.

Table 1. *Crystallographic data for* $Ca_4YFe_5O_{13}$

Symmetry	Orthorhombic
Lattice parameters	$a = 5{\cdot}46$, $b = 37{\cdot}4$, $c = 5{\cdot}54$ Å
Systematic absences	$0kl$ with $k + l = 2n + 1$ $hk0$ with $h = 2n + 1$
Possible space groups	$Pn2_1a$ or $Pnma$
Z	4
D_{calc}	4·326 Mg m^{-3}

Table 2. *Symmetries of CBED patterns for the two space groups Pnma and* $Pn2_1a$

Space group	Point group	Zone axis	Diffraction group	Whole pattern
Pnma	*mmm*	[010]	$2mm1_R$	*2mm*
		[10$\bar{1}$]	2_Rmm_R	*m*
$Pn2_1a$	*m2m*	[010]	*2mm*	*2mm*
		[10$\bar{1}$]	m_R	1

groups are non-centrosymmetric $Pn2_1a$ or centrosymmetric *Pnma*. The crystallographic data of $Ca_4YFe_5O_{13}$ are summarized in Table 1.

Figs. 2(*a*) and (*b*) show the CBED patterns taken along the [010] and [10$\bar{1}$] zone axes, respectively. In order to interpret the symmetry of the CBED patterns, it is helpful to show the relation between the point group, diffraction group and the symmetry of the CBED pattern, which is given by Buxton *et al.* (1976). Table 2 shows the two point groups for the $Pn2_1a$ and *Pnma* space groups and the corresponding diffraction groups for the zone-axis setting and the whole symmetry of the CBED patterns. From the inspection of the CBED pattern of Fig. 2(*a*), it is known that two mirror lines which are perpendicular to each other are present in the whole pattern. This means that the whole symmetry has *2mm*. The CBED pattern of Fig. 2(*b*), in which each disk of the CBED patterns is overlapped because of the long *b* axis, suggests that the whole pattern shows the presence of *m* symmetry which is perpendicular to the b^* axis. These results indicate that the present crystal belongs to the point group *mmm*. Therefore the true space group must be centrosymmetric *Pnma*.

It is interesting to note in Fig. 2(*a*) that *2mm* symmetry shows a dark band along the a^* axis in alternate reflections such as the 100 and $\bar{1}00$. As pointed out by Gjønnes & Moodie (1965), such reflections are kinematically forbidden reflections as a result of the presence of a screw axis or a glide plane. In the present case, the dynamic absence is coming from the presence of the *a*-glide plane parallel to the incident beam diffraction.

2. 1 MeV *high-resolution electron microscopy*

Fig. 3 shows a structure image of a $Ca_4YFe_5O_{13}$ crystal taken from a very thin region. The incident electron beam was parallel to the [10$\bar{1}$] direction. The corresponding diffraction pattern is shown in Fig. 1(*a*), in which the size and the position of the objective aperture is outlined. About 60 waves were used for imaging. The image contrast consists of the arrangements of dark dots and white spots. As pointed out in the previous observations (Bando, Watanabe, Sekikawa, Goto & Horiuchi, 1979; Bando, Watanabe & Sekikawa, 1979, 1980), each cation site should be resolved as a dark dot in the 1 MeV structure image if the metal-to-metal distance is larger than about 2 Å in the projected plane. Based on this analogy, the dark dots are assigned as Y, Ca and Fe cations. It is then clear that the arrangement of the dark dots can be interpreted intuitively on the basis of the known crystal structure of $Ca_2Fe_2O_5$ (Berggren, 1971), in which the structure consists of alternate stacking of FeO_6 octahedra (*O* layer) and FeO_4 tetrahedra (*T* layer) along

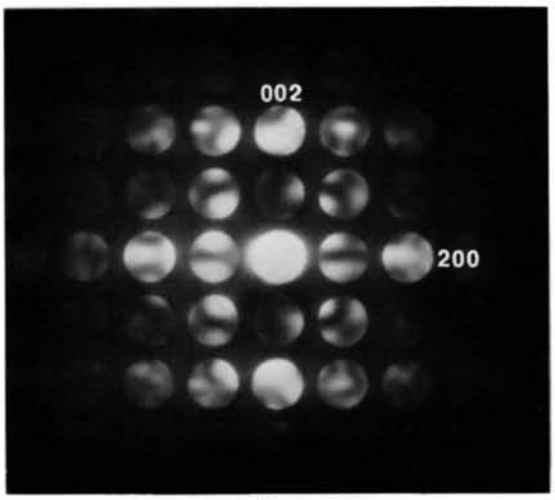

(*a*)

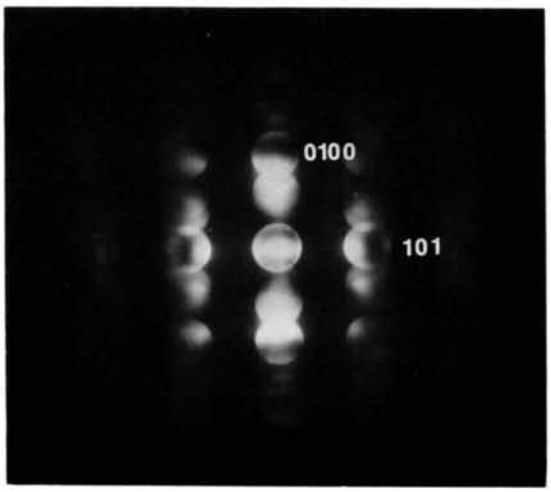

(*b*)

Fig. 2. Convergent-beam electron diffraction patterns. (*a*) [010] and (*b*) [101] zone-axis patterns, showing the whole pattern symmetry.

the *b* axis. The proposed crystal structure of $Ca_4YFe_5O_{13}$ read from the image is inserted in the figure. The structure is built up of a stacking sequence of ...*OTOOTOTOOTO*... along the *b* axis at intervals of 37·4 Å.

It should be noted in Fig. 3 that the arrangement of cation atoms shows the presence of mirror symmetry perpendicular to the *b* axis. This implies that the present crystal belongs to centrosymmetric *Pnma*, which is consistent with the result of the CBED patterns described in § 1.

A structure image taken from the [100] zone axis is shown in Fig. 4, and the corresponding diffraction pattern is shown in Fig. 1(*b*). The structure model projected onto the (100) plane is illustrated in the figure. In this projection, the dark dots are arranged almost parallel to the *b* axis. Because the distances between cations are as small as 1·8 to 2·0 Å, each dot is not resolved separately, forming the dark line along the *b* axis.

In order to interpret the observed images exactly, the image contrast was calculated for a proposed crystal structure, which will be described later, by means of the multi-slice method derived by Cowley & Moodie (1957). The slice thickness was 7·6 and 5·46 Å and the interaction of 253 and 305 waves was taken into account for the images projected onto the [10$\bar{1}$] and [100] zone axes, respectively. The image contrast was then computed with the experimental values; the accelerating voltage was 800 keV, the spherical abberation constant was 10 mm, and the aperture size was 0·5 $Å^{-1}$ in reciprocal space.

The calculated images for the [10$\bar{1}$] and [100] directions are shown in the inserts of Figs. 3 and 4, respectively, for a crystal thickness of about 40 Å and at an underfocus of 1000 Å. It is clear that each cation site appears as a dark dot. The calculated images agree well with observed images suggesting that straightforward interpretation is valid for the present observation.

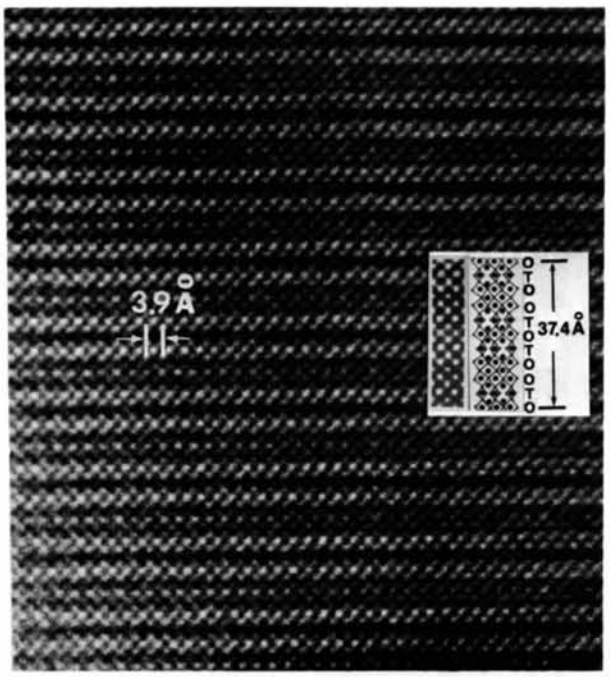

Fig. 3. A structure image of $Ca_4YFe_5O_{13}$. The incident electron beam is parallel to [10$\bar{1}$]. The proposed crystal structure is inserted in the figure, in which dark circles stand for cubo-octohedral Y, Ca atoms and octahedral and tetrahedral Fe atoms, while open circles stand for oxygen atoms. The calculated image is shown in the inset, obtained at a crystal thickness of about 40 Å and underfocus of 1000 Å. The structure consists of the stacking sequence of FeO_6 octahedra (*O* layer) and FeO_4 tetrahedra (*T* layer), and is represented by the stacking sequence of ...*OTOOTOTOOTO*... along the *b* axis at intervals of 37·4 Å.

Description of the structure

The crystal structure of $Ca_4YFe_5O_{13}$ which is projected onto the (100) plane is shown in Fig. 5(*a*), in which the iron and oxygen atoms are indicated by dark circles and open circles, respectively. The quadrilaterals and triangles stand for the FeO_6 octahedra and the FeO_4 tetrahedra, respectively. The crystallographically non-equivalent positions and the site of the mirror plane are

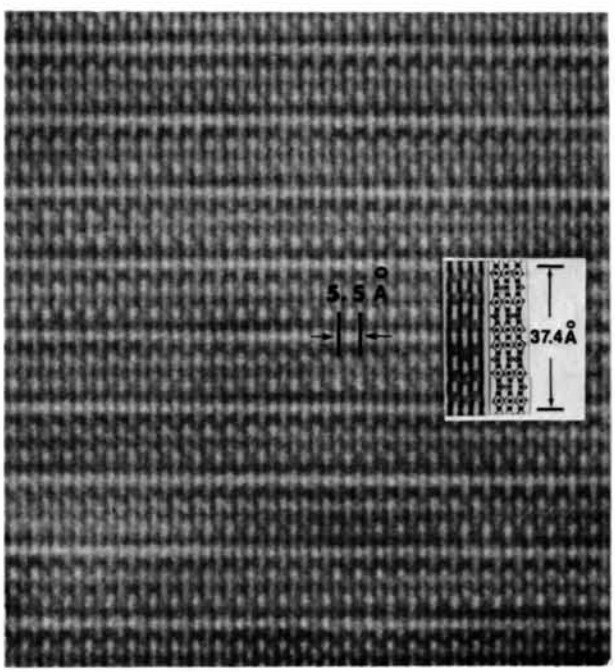

Fig. 4. A structure image of $Ca_4YFe_5O_{13}$ taken along the [100] direction. The corresponding diffraction pattern is shown in Fig. 1(*b*). The structure model is inserted, in which symbols are the same as those in Fig. 3. The calculated image is shown in the inset, obtained at a crystal thickness of about 40 Å and underfocus of 1000 Å.

shown. The crystal contains four molecular units. The cubooctahedral cation sites occupied by the Y and Ca atoms are abbreviated for simplicity in the figure. The structure is built up of a succession of FeO_6 octahedra and FeO_4 tetrahedra and consists of six octahedral layers and four tetrahedral layers, forming the stacking sequence ...*OTOOTOTOOTO*... along the *b* axis at intervals of 37·4 Å. The chemical composition of the present crystal is determined from the structure model.

In order to compare the present crystal structure with that of dicalcium ferrite $Ca_2Fe_2O_5$ which has been determined by Berggren (1971), the structure of $Ca_2Fe_2O_5$ is shown in Fig. 5(*b*). This crystal is orthorhombic with unit-cell dimensions $a = 5{\cdot}43$, $b = 14{\cdot}8$ and $c = 5{\cdot}6$ Å, and the space group is *Pnma*. The structure is built up of an alternate stacking of the FeO_6 octahedra and the FeO_4 tetrahedra and is represented as ...*OTOTO*... along the *b* axis at intervals of 14·8 Å. The FeO_6 octahedra are tilted by about 11° with respect to the *b* axis. The mirror plane perpendicular to the *b* axis is situated within the FeO_4 tetrahedral layer.

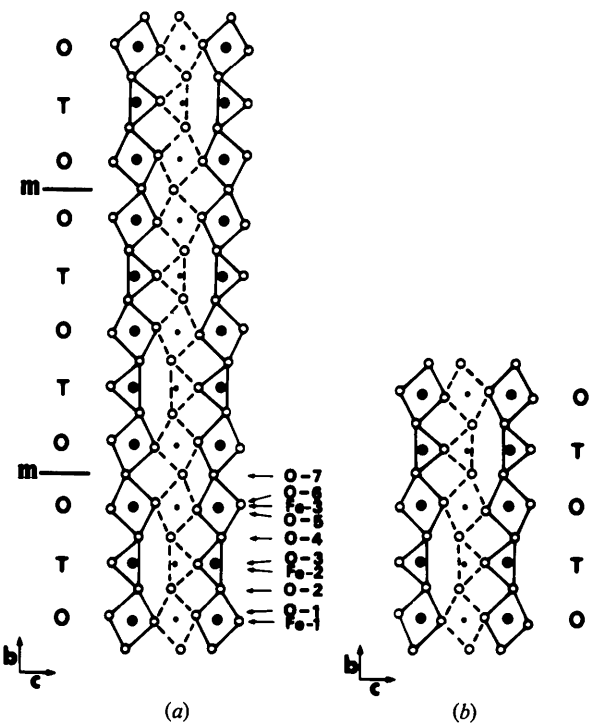

(*a*) (*b*)

Fig. 5. (*a*) A structure model of $Ca_4YFe_5O_{13}$. The iron and oxygen are shown by dark circles and open circles, respectively. The quadrilaterals and triangles indicate FeO_6 octahedra (*O* layer) and FeO_4 tetrahedra (*T* layer), respectively, at $a = 0$ and the quadrilaterals and triangles which are shown with broken lines indicate octahedra and tetrahedra, respectively, at $a = \frac{1}{2}$. The crystallographic non-equivalent positions and the site of the mirror plane are also shown. The cubooctahedral sites are omitted for simplicity. The structure is built up from the stacking sequence of ... *OTOOTOTOOTO* ... along the *b* axis at intervals of 37·4 Å. (*b*) The crystal structure of $Ca_2Fe_2O_5$ (Berggren, 1971). The structure consists of an alternate stacking of FeO_6 octahedra and FeO_4 tetrahedra and is represented by the stacking sequence ...*OTOTO*... along the *b* axis at intervals of 14·8 Å.

Table 3. *Atomic parameters of* $Ca_4YFe_5O_{13}$

Atom	Position	*x*	*y*	*z*
Ca(1)	8(*d*)	0·50	0·05	0·00
Ca(2)	8(*d*)	0·50	0·15	0·00
Y	4(*c*)	0·50	$\frac{1}{4}$	0·0
Fe(1)	4(*a*)	0	0	0
Fe(2)	8(*d*)	0·00	0·10	0·00
Fe(3)	8(*d*)	0·00	0·20	0·00
O(1)	8(*d*)	0·25	0·00	0·25
O(2)	8(*d*)	0·00	0·05	0·10
O(3)	8(*d*)	0·60	0·10	−0·10
O(4)	8(*d*)	0·00	0·15	0·10
O(5)	8(*d*)	0·25	0·20	0·25
O(6)	8(*d*)	0·25	0·20	0·25
O(7)	4(*c*)	0·00	$\frac{1}{4}$	−0·10

By comparing these two structures, it is understood that the structure of the $Ca_4YFe_5O_{13}$ crystal can be described in terms of unit-cell twinning of the $Ca_2Fe_2O_5$ crystal. In the $Ca_4YFe_5O_{13}$ crystal, the twin plane is (010) and the twin boundary is located at the midpoint of the perovskite slab (*O–O* double layers). The trivalent Y cations are at the twin boundary. The approximate atomic parameters of the $Ca_4YFe_5O_{13}$ crystal are then assigned on the basis of those in $Ca_2Fe_2O_5$ and are given in Table 3, in which numbers of non-equivalent positions and symmetry positions are indicated.

It is generally difficult to estimate the accuracy of the structure determination by the high-resolution electron microscopy method, because it depends on the image resolution obtained. In the present case, each of the heavy-metal-atom sites is clearly resolved in the image. Therefore, the accuracy of these atom coordinates is rather high. On the other hand, the coordinates of the oxygen atoms are only assigned by speculation from a crystal-chemical consideration on the basis of the related crystal structure, because the oxygen atoms do not show any contrast in the image. Their accuracy must be low. However, the present high-resolution electron microscopy method is very useful to determine the approximate arrangement of frameworks. The coordinates roughly estimated from this method should be suitable as starting data for future X-ray or neutron diffraction methods.

The authors would like to express deep gratitude to Professor J. M. Cowley and Dr S. Iijima at Arizona State University for valuable discussions and for correcting the manuscript. They thank Dr J. W. Steeds, University of Bristol, for valuable discussions.

Part of the present work was supported by NSF grants DMR 80-15785 and by the Facility for High-Resolution Electron Microscopy, established with support from the NSF Regional Instrumentation Facilities Program.

References

BANDO, Y., SAEKI, Y., SEKIKAWA, Y., MATSUI, Y., HORIUCHI, S. & NAKAHIRA, M. (1979). *Acta Cryst.* A**35**, 564–569.

BANDO, Y., WATANABE, M. & SEKIKAWA, Y. (1979). *Acta Cryst.* B**35**, 1541–1545.

BANDO, Y., WATANABE, M. & SEKIKAWA, Y. (1980). *J. Solid State Chem.* **33**, 413–419.

BANDO, Y., WATANABE, M., SEKIKAWA, Y., GOTO, M. & HORIUCHI, S. (1979). *Acta Cryst.* A**35**, 142–145.

BANDO, Y., YAMAMURA, H. & SEKIKAWA, Y. (1980). *J. Less-Common Met.* **70**, 281–284.

BERGGREN, J. (1971). *Acta Chem. Scand.* **25**, 3616–3624.

BUXTON, B. F., EADES, J. A., STEEDS, J. W. & RACKHAM, G. M. (1976). *Philos. Trans. R. Soc. London Ser. A*, **281**, 171–194.

COWLEY, J. M. & MOODIE, A. F. (1957). *Acta Cryst.* **10**, 609–619.

GJØNNES, J. & MOODIE, A. F. (1965). *Acta Cryst.* **19**, 65–67.

GOODMAN, P. (1975). *Acta Cryst.* A**31**, 804–810.

GOODMAN, P., SPENCE, J., OLSEN, A. & ROTH, R. (1980). *38th Annual EMSA*, p. 174.

GRENIER, J. C., DARRIET, J., POUCHARD, M. & HAGENMULLER, P. (1976). *Mater. Res. Bull.* **11**, 1219–1226.

GRENIER, J. C., SCHIFFMACHER, G., CARO, P., POUCHARD, M. & HAGENMULLER, P. (1979). *J. Solid State Chem.* **20**, 365–379.

HORIUCHI, S., KIKUCHI, T. & GOTO, M. (1977). *Acta Cryst.* A**33**, 701–703.

HORIUCHI, S., MATSUI, Y. & BANDO, Y. (1976). *Jpn. J. Appl. Phys.* **15**, 2483–2484.

JOHNSON, A. W. S. & GATEHOUSE, B. M. (1980). *Acta Cryst.* B**36**, 523–526.

MATSUI, Y., KATO, K., KIMIZUKA, N. & HORIUCHI, S. (1979). *Acta Cryst.* B**35**, 561–564.

TANAKA, M., SAITO, R. & WATANABE, D. (1980). *Acta Cryst.* A**36**, 350–352.

Acta Cryst. (1981). A**37**, 728–734

Energy Analyses for the Alkaline-Earth Formates

BY MASANORI MATSUI

Chemical Laboratory, Kanazawa Medical University, Uchinada, Ishikawa-ken 920-02, *Japan*

AND TOKUNOSUKÉ WATANABÉ

Osaka University, Yamada, Suita 565, *Japan*

(*Received* 24 *January* 1981; *accepted* 24 *March* 1981)

Abstract

The structures of the alkaline-earth formates have been investigated in terms of lattice energy calculations. The lattice energy E was approximated to be the sum of electrostatic and repulsive terms, where the repulsive potential used was in the form: $(1/12)f(R_\alpha + R_\beta)^{13} r^{-12}$ (r, interatomic distance; f, arbitrarily chosen standard force; R_α, repulsive radius of an atom α). The potential parameters concerned were obtained with the structures of α-$Ca(HCOO)_2$, α-$Sr(HCOO)_2$ and $Ba(HCOO)_2$. These potential parameters were successfully used for the determination of the structure of β-$Sr(HCOO)_2$, for the differentiation of the structures of α-$Sr(HCOO)_2$ and $Ba(HCOO)_2$, and for the interpretation of the large anisotropy of thermal vibrations in β-$Ca(HCOO)_2$.

Introduction

The crystal structures of the alkaline-earth formates are manifold. They can be shown by the following scheme, where each box stands for a type of crystal structure.

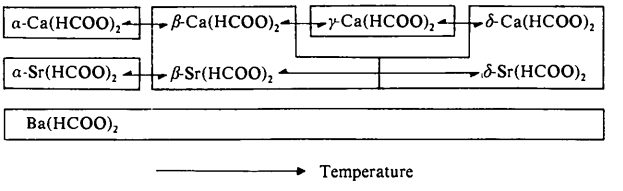

Thus, the isomorphism does not hold for α-$Ca(HCOO)_2$, α-$Sr(HCOO)_2$ and $Ba(HCOO)_2$, which are the stable modifications at room temperature under atmospheric pressure (Watanabé & Matsui, 1978). β-$Ca(HCOO)_2$ and β-$Sr(HCOO)_2$ and δ-$Ca(HCOO)_2$

0567-7394/81/050728-07$01.00